Molecular and Physical Composition of Tar Balls in Wildfire Smoke: An Investigation with Complementary Ionisation Methods and 15-Tesla FT-ICR Mass Spectrometry

Amna Ijaz,*†[a] William Kew,[b] Zezhen Cheng,[b] Susan Mathai,[c,d] Nurun Nahar Lata,[b] Libor Kovarik,[b] Simeon Schum,[a] Swarup China,[b] and Lynn R. Mazzoleni,*[a,d]

[a.] Department of Chemistry, Michigan Technological University, Houghton, Michigan 49931, USA.
[b.] Environmental Molecular Sciences Laboratory, Pacific Northwest National Laboratory, Richland 99354, WA USA.
[c.] Department of Physics, Michigan Technological University, Houghton 49931 MI, USA.
[d.] Atmospheric Sciences Program, Michigan Technological University, Houghton 49931 MI, USA

†Present address: Laboratoire Chimie Environnement, Aix-Marseille Université, Marseille 13005, France
* Corresponding authors: aijaz@mtu.edu and lrmazzol@mtu.edu.

SUPPLEMENTARY TABLES

Table S1. Equations/models used to compute physicochemical parameters from formulae assigned to high-resolution mass spectrometric data

Parameter	Equation	Reference
Modified aromaticity index	$AI_{mod} = \dfrac{1 + C - 0.5(O) - S - 0.5(H) - 0.5(N) - 0.5(P)}{C - 0.5(O) - S - N - P}$	1, 2

C, O, S, H, and N are the numbers of atoms of these elements in each molecular formula. $AI_{mod} \leq 0$ were categorised as aliphatic; $0 < AI_{mod} \leq 0.5$ and O/C < 0.5 were classified as unsaturated with low O; $0 < AI_{mod} \leq 0.5$ and O/C > 0.5 were classified as unsaturated with high O; $0.5 < AI_{mod} < 0.67$ were classified as aromatic, and $AI_{mod} \geq 0.67$ were classified as condensed aromatic.

Parameter	Equation	Reference
Saturation mass concentration	$log_{10}C_0 = (n^0C - C) \times bC - O \times bO - H \times bH - 2 \times ((C \times O)/(C + O)) \times bCO - N \times bN - S \times bS$	3

C, O, S, H, and N are the numbers of atoms of these elements in each molecular formula. n^0C is the reference C number; bC, bO, bN, and bS denote the contribution of each atom to the estimated C^0. bCO is the C-O non-ideality coefficient. The values of these constants are different based on molecular groups to which a given formula belongs (CHO, CHNO, CHOS, CH, CHNOS, or CHN) and were accessed from the report published by Li et al., 2016[3]. Formulae with $log_{10}C_0 \leq$ -3.52 were categorised as extremely low volatility (ELVOC), $-3.52 < log_{10}C_0 \leq -0.52$ as low volatility (LVOC), $-0.52 < log_{10}C_0 \leq 2.47$ as semi-volatile (SVOC), $2.47 < log_{10}C_0 \leq 6.47$ as intermediate volatility (IVOC), and those with $6.47 < log_{10}C_0$ as volatile organic compounds (VOC).
The values of coefficients were originally described in Li et al., 2016[3] and are also summarised below.

Classes	n^0C	b_C	b_H	b_O	b_{CO}	b_N	b_S
CH	17.95	0.5742	-0.1417	--	--	--	--
CHO	15.77	0.6238	-0.1387	1.735	-0.8592	--	--
CHN	23.01	0.4307	-0.02110	--	--	0.9528	--
CHNO	21.12	0.4139	-0.03760	0.8092	-0.1174	1.1010	--
CHOS	16.07	0.5348	-0.1507	1.354	-0.4175	--	0.8993
CHNOS	19.20	0.5469	0.1368	1.183	0.07310	1.0289	1.323

Parameter	Equation	Reference
Dry glass transition temperature	$T_{g,dry} = (n^0C + logC)bC + (logH \times bH) + (logC \times logH \times bCH) + (logO \times bO) + (logC \times logO$	4

n^0C is the reference C number, bC, bH, and bO represent the numeric contribution of these elements to $T_{g,dry}$. Also, bCH and bCO are coefficients that reflect contributions from C-H and C-O bonds, respectively. This equation is applicable to CHO species only. The values of these constants were accessed from the report published by DeRieux et al., 2018[4].
The values of coefficients were originally described in DeRieux et al., 2018[4] and are also summarised below.

Classes	n^0C	b_C	b_H	b_{CH}	b_O	b_{CO}
CH	1.96	61.99	−113.33	28.74	--	--
CHO	12.13	10.95	−41.82	21.61	118.96	−24.38

Parameter	Equation	Reference
Relative humidity-dependent glass transition temperatures	$T_{g,RH} = \dfrac{(1 - w_{org})T_{g,w} + \left(\dfrac{1}{K_{gt}} \times w_{org} \times T_{g,dry}\right)}{(1 - w_{org}) + \left(\dfrac{1}{K_{gt}} \times w_{org}\right)}$ $w_{org} = \dfrac{1.4 - \left((1.4 \times RH)/100\right)}{1.4 - \left((1.28 \times RH)/100\right)}$	5
Phase state ratio (PSR)	$T_{g,RH}/T_{amb}$	

$T_{g,w}$ is the glass transition temperature of water, i.e., 136 K, and K_{gt} is the Gordon-Taylor constant that is equal to 2.5 ± 1.5. Here, RH is the measured relative humidity on the day of sampling in Richland, WA. Meteorological conditions are presented in Table S1. Tamb is the ambient temperature recorded on the day of sampling. Species with PSR of ≥ 1 are projected to exist as solids, 1.0 ≥ PSR ≥ 0.8 as semi-solids, and PSR ≤ 0.8 as liquids.

Table S2 Summary of average chemical characteristics of aerosol mixtures inferred from <u>all</u> molecular species detected by negative-ion electrospray ionisation coupled to 15-T FT-ICR MS. All averages are weighted to normalised abundance. For a summary derived from species exclusively detected in each sample please refer to Table 2. Standard deviations are given in brackets.

Aerosol mixture	Molecular group	MF	O/C$_{wa}$	H/C$_{wa}$	DBE$_{wa}$	AI$_{mod,wa}$	T$_{g,RH}$* (K)
					ESI		
BBAug09(DT)	All	3663	0.68 (0.18)	1.16 (0.28)	7.44 (3.06)	0.24 (0.26)	--
	CHO	1847	0.68 (0.17)	1.14 (0.27)	7.39 (2.93)	0.26 (0.20)	313.92 (272.35)
	CHNO	1608	0.68 (0.16)	1.16 (0.28)	8.29 (2.96)	0.22 (0.20)	--
	CHOS	208	1.00 (0.27)	1.62 (0.20)	2.89 (1.20)	0.12 (0.87)	--
BBAug0910(NT)	All	3686	0.69 (0.17)	1.25 (0.29)	6.60 (2.79)	0.20 (0.27)	--
	CHO	1554	0.67 (0.16)	1.19 (0.27)	6.69 (2.70)	0.23 (0.20)	308.13 (269.98)
	CHNO	1876	0.70 (0.19)	1.30 (0.30)	6.97 (2.76)	0.15 (0.22)	--
	CHOS	256	0.96 (0.26)	1.63 (0.19)	2.90 (1.22)	0.10 (0.80)	--
BBAug1011	All	3922	0.68 (0.20)	1.25 (0.29)	6.63 (2.92)	0.21 (0.41)	--
	CHO	1734	0.65 (0.16)	1.20 (0.26)	6.76 (2.76)	0.23 (0.19)	304.65 (265.93)
	CHNO	1865	0.68 (0.20)	1.27 (0.30)	7.36 (2.89)	0.20 (0.62)	--
	CHOS	323	0.94 (0.26)	1.62 (0.21)	2.95 (1.27)	0.09 (0.74)	--
BBAug1314	All	4841	0.67 (0.21)	1.17 (0.29)	7.46 (3.21)	0.25 (0.32)	--
	CHO	2221	0.65 (0.19)	1.12 (0.27)	7.50 (3.14)	0.28 (0.20)	303.85 (266.34)
	CHNO	2366	0.67 (0.21)	1.22 (0.28)	7.97 (3.05)	0.20 (0.31)	--
	CHOS	254	1.01 (0.31)	1.63 (0.26)	2.64 (1.35)	0.19 (1.04)	--

Table S3 Summary of average chemical characteristics of aerosol mixtures inferred from <u>all</u> molecular species detected by negative-ion laser desorption ionisation coupled to 15-T FT-ICR MS. All averages are weighted to normalised abundance. For a summary derived from species exclusively detected in each sample please refer to Table 3. Standard deviations are given in brackets.

Aerosol mixture	Molecular group	MF	O/C$_{wa}$	H/C$_{wa}$	DBE$_{wa}$	AI$_{mod,wa}$	T$_{g,RH}$* (K)
					LDI*		
BBAug0910(NT)	All	1516	0.48 (0.21)	1.06 (0.33)	7.12 (2.95)	0.40 (0.25)	--
	CHO	967	0.50 (0.21)	1.10 (0.34)	6.76 (2.95)	0.37 (0.25)	280.04 (253.69)
	CHNO	523	0.43 (0.17)	0.94 (0.25)	8.11 (2.35)	0.50 (0.22)	--
	CHOS		Not detected/assigned a formula above the S/N				
BBAug1011	All	2383	0.53 (0.21)	1.01 (0.31)	7.88 (3.11)	0.41 (0.24)	--
	CHO	1447	0.54 (0.22)	1.04 (0.32)	7.54 (3.18)	0.38 (0.25)	286.25 (254.83)
	CHNO	928	0.48 (0.17)	0.92 (0.24)	8.89 (2.58)	0.49 (0.22)	--
	CHOS		Not detected/assigned a formula above the S/N				
BBAug1314	All	4299	0.59 (0.26)	1.01 (0.30)	8.87 (3.59)	0.40 (0.44)	--
	CHO	2281	0.56 (0.22)	0.99 (0.29)	8.89 (3.51)	0.40 (0.23)	297.65 (262.78)
	CHNO	1581	0.51 (0.18)	0.94 (0.24)	10.01 (3.07)	0.44 (0.22)	--
	CHOS	423	1.09 (0.30)	1.40 (0.26)	4.38 (2.05)	0.28 (1.42)	--

*Two additional molecular groups: CH and CHN were detected here with formulae forming only <1% of all assignments, and hence, have been omitted from this summary.
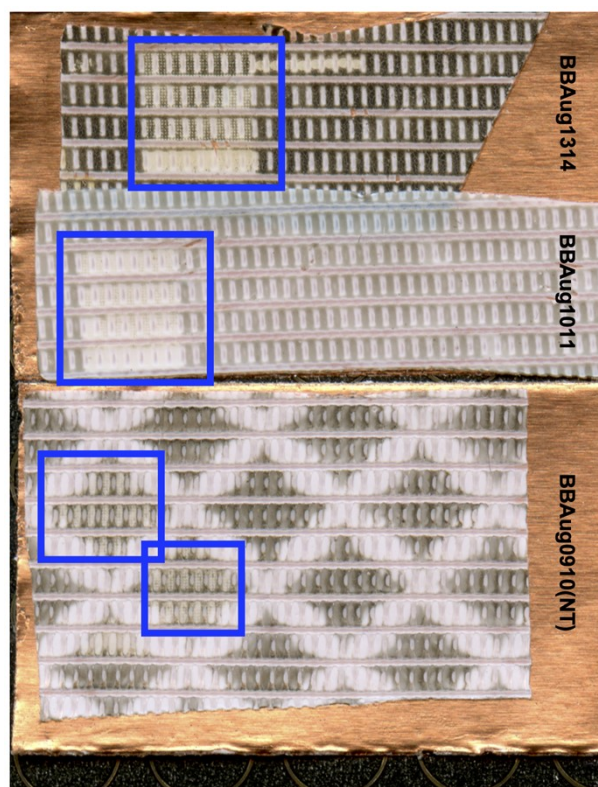
SUPPLEMENTARY FIGURES

Fig. S1 Small strips of aerosol-loaded filters pasted on a double-sided copper tape affixed on a polished steel matrix-assisted laser desorption ionisation (MALDI) plate. Blue frames indicate portions of the substrate from where the sample was ablated due to laser impact (Photograph courtesy of Dr William Kew, Environmental Molecular Sciences Laboratory, Pacific Northwest National Laboratory, WA, USA).
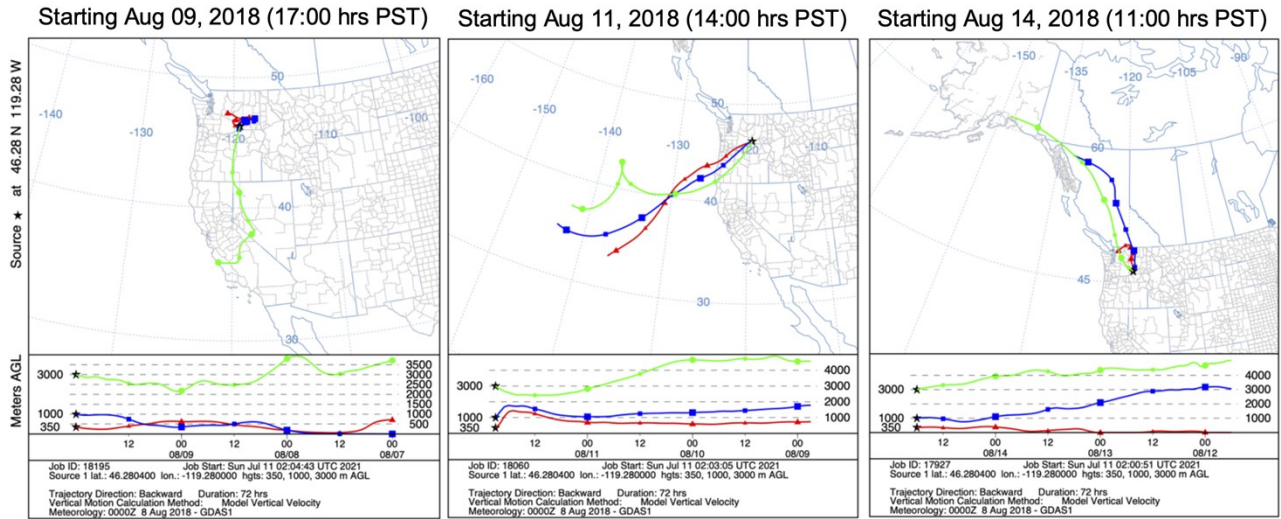
Fig. S2 Backward trajectories extending 72 hours from the time that sample collection was concluded were modelled using the Hybrid Single-Particle Lagrangian Integrated Trajectory (HYSPLIT) at heights of 350 (red), 1000 (blue), and 3000 (green) meters above ground level. Star denotes the site of sample collection at 46.28° N and -119.28° W.
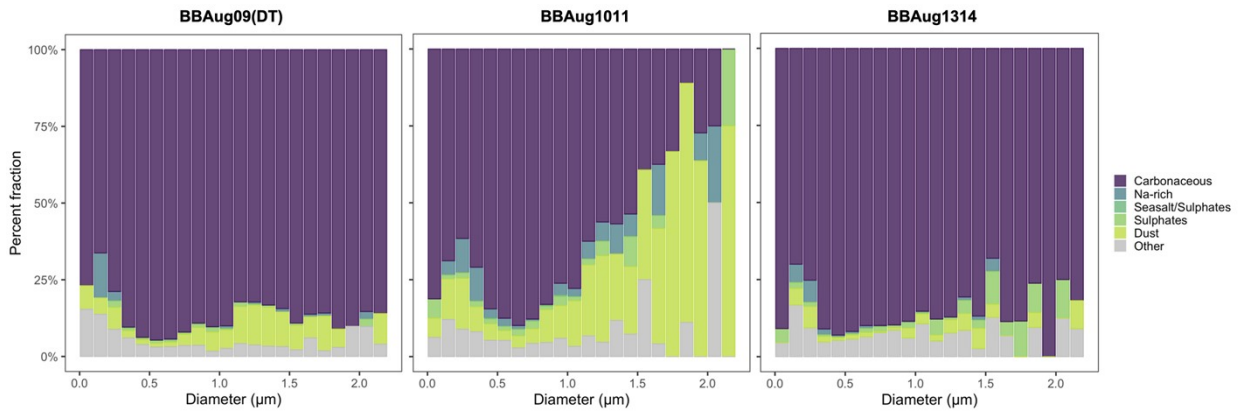
Fig. S3 Size-resolved particle composition of the non-tar ball (BBAug09(DT) and BBAug1011) and tar ball-rich (BBAug1314) aerosol from computer-controlled scanning electron microscopy and electron-dispersive X-ray spectroscopy analyses.
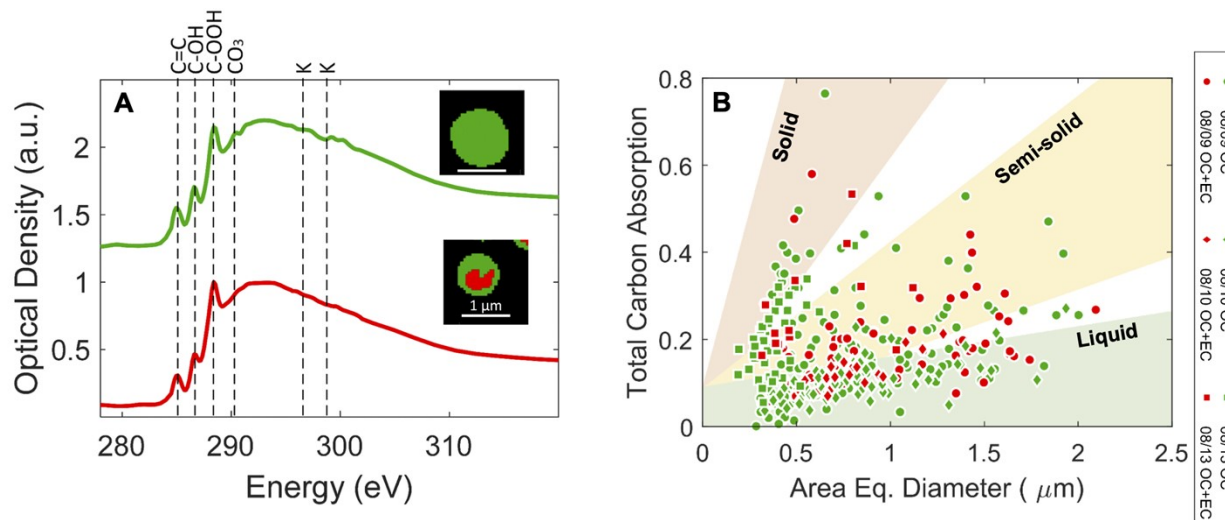
Fig. S4 The optical thickness of representative single particles, (A) Carbon K-edge absorption spectra from scanning transmission electron microscopy (STXM) and near-edge X-ray absorption fine structure spectroscopy (STXM/NEXAFS) analysis of two types of particles in the TB-rich aerosol, BBAug1314: pure organic carbon (OC; green) and organic carbon with elemental carbon inclusions (OC + EC; red). Major absorption peaks correspond to sp^2, ketonic, hydroxyl, and carboxyl functionalities. A minor carbonate (inorganic C) peak is seen for the BBAug1314 sample, (B) Total carbon absorption as a function of particle size. Colours represent the type of particle, i.e., only OC (green) or OC + EC (red). Shape denotes aerosol samples on different days. Phase state boundaries show BBAug1314 to have a prevalence of OC-only particles that accumulate in a zone of solid small-diameter particles of relatively higher optical thickness, especially those with no EC inclusions. Both non-TB aerosols have more particles of OC + EC type and accumulate in regions of lower optical thickness.
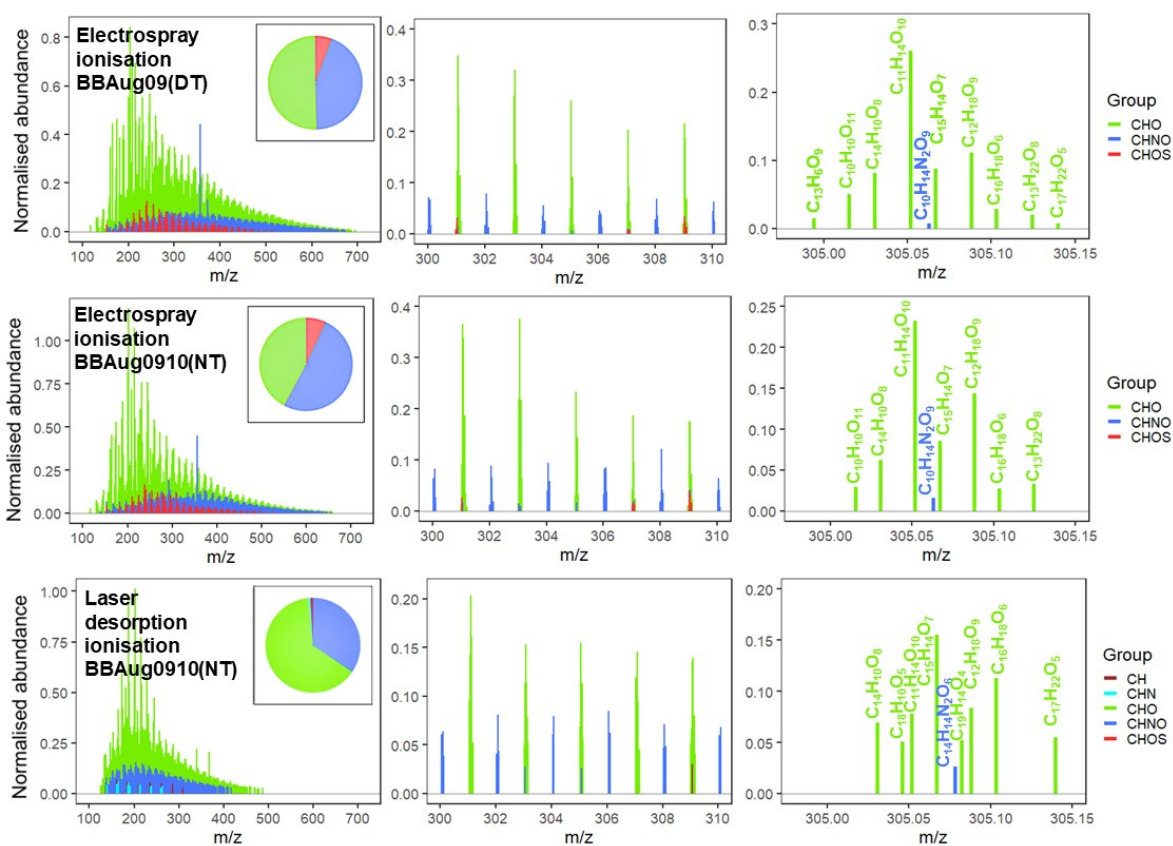
Fig. S5 Reconstructed stick mass spectra for non-TB aerosol acquired with negative-ion laser desorption or electrospray ionisation with 15-T FT-ICR mass spectrometry. Only monoisotopic peaks are shown. Peak abundances are normalised to the sum of the abundance of CHO species that were common among ≥(n-1) samples, where n is the total number of samples under consideration. Pie charts show the fraction of molecular formulae belonging to CHO (green), CHNO (blue), and CHOS (red) groups. Corresponding numerical data is presented in Tables S2 and S3. No spectra could be obtained for BBAug09(DT) with (-)LDI.
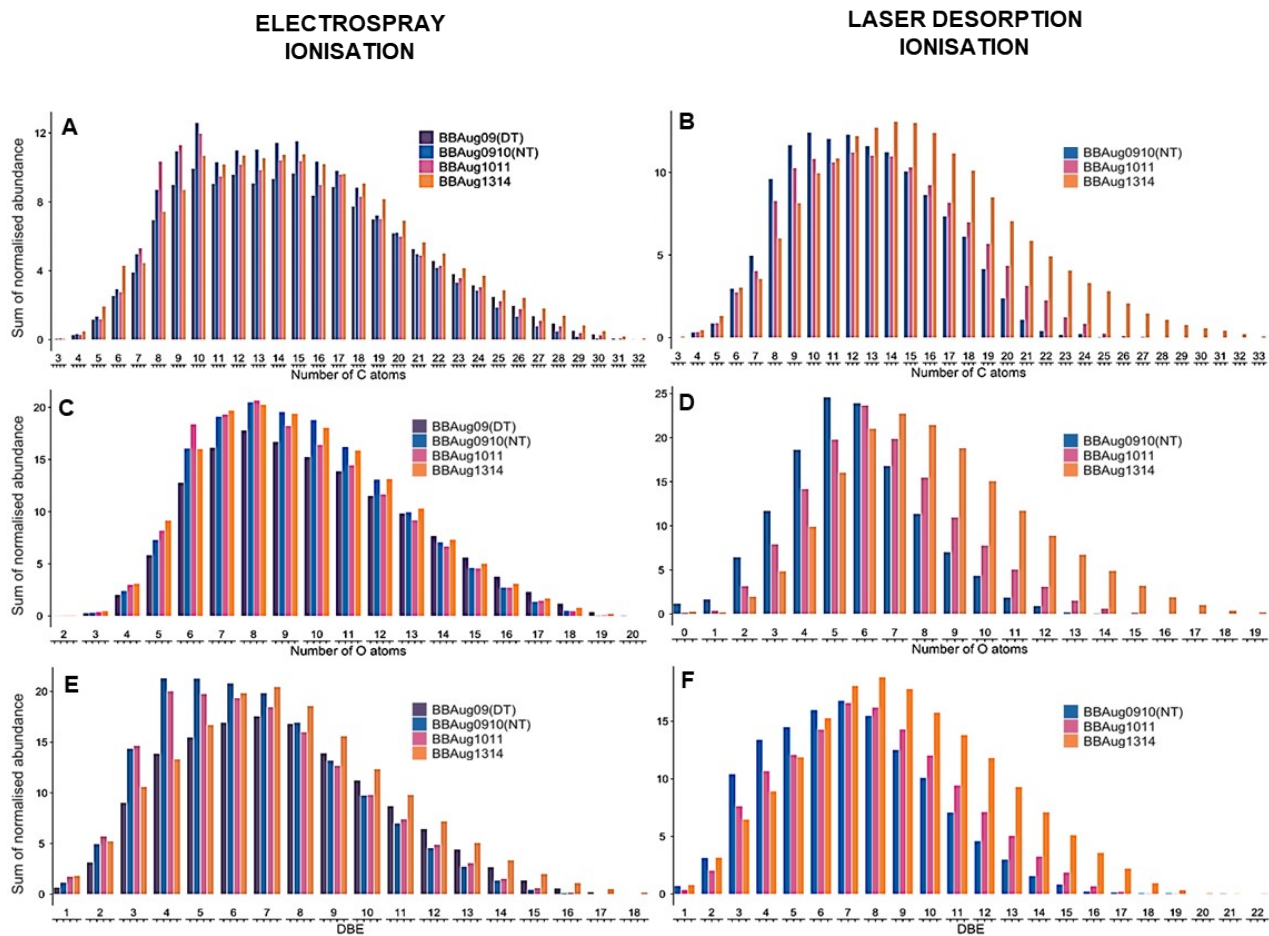
Fig. S6 Distribution of ion abundance across molecular formulae with all observed (A-B) number of carbon atoms, (C-D) number of oxygen atoms, and (E-F) double bond equivalence with negative-ion laser desorption or electrospray ionisation / 15-T FT-ICR MS analysis
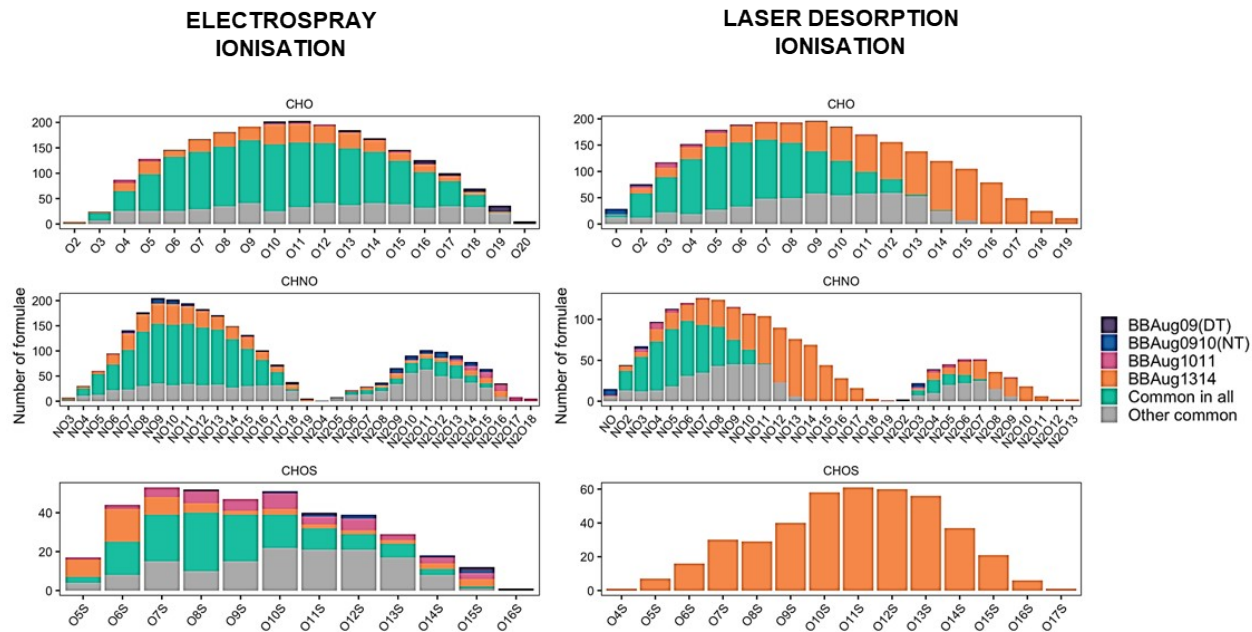
Fig. S7 Distribution of molecular formulae across classes with all combinations of C, H, O, N, and S observed with negative-ion laser desorption or electrospray ionisation / 15-T FT-ICR MS analysis
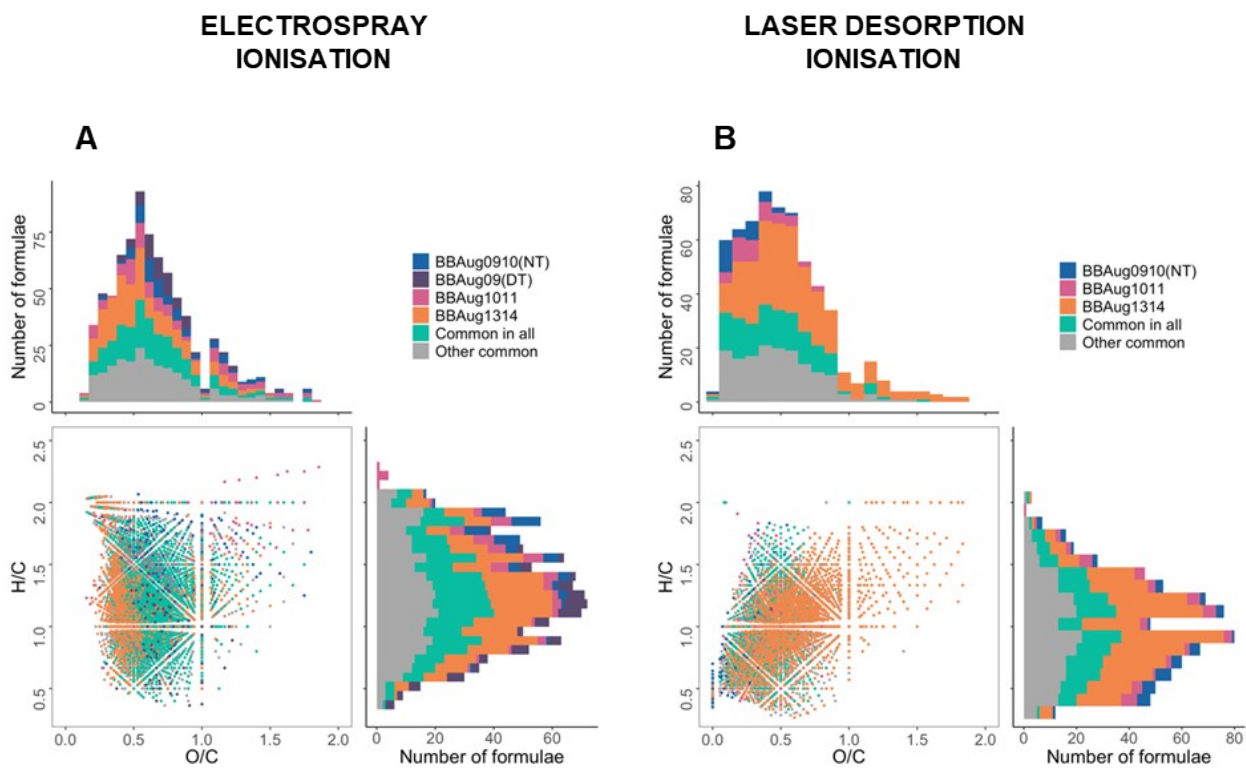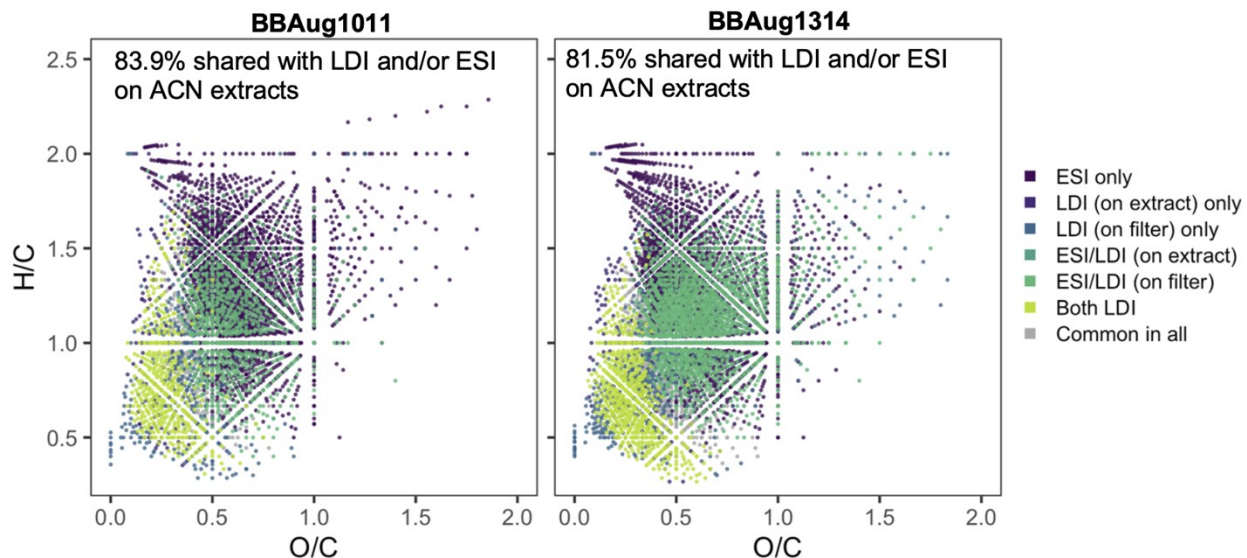
Fig. S8. Van Krevelen diagrams exhibiting the molecular formulae commonly or exclusively identified in the aerosol samples. Histograms have been drawn to better visualise overlapping data points.

	BBAug1011			BBAug1013		
	MF	O/C$_{avg}$	H/C$_{avg}$	MF	O/C$_{avg}$	H/C$_{avg}$
ESI	3922	0.68 ± 0.20	1.25 ± 0.29	4841	0.67 ± 0.21	1.17 ± 0.29
LDI$_{extract}$	1095	0.39 ± 0.16	0.92 ± 0.32	1533	0.40 ± 0.16	0.80 ± 0.24
LDI	2383	0.53 ± 0.21	1.01 ± 0.31	4299	0.59 ± 0.26	1.01 ± 0.30
Species exclusively detected by each ionisation method and in all possible combinations						
ESI	2402	0.69 ± 0.23	1.36 ± 0.31	1982	0.64 ± 0.24	1.35 ± 0.34
LDI$_{extract}$	71	0.21 ± 0.08	1.09 ± 0.47	66	0.23 ± 0.12	0.98 ± 0.37
LDI	135	0.42 ± 0.30	0.85 ± 0.45	794	0.55 ± 0.36	0.98 ± 0.34
ESI/LDI$_{extract}$	1	0.25	1.88	2	0.78 ± 0.55	1.01 ± 0.45
ESI/LDI	573	0.63 ± 0.19	1.16 ± 0.29	2040	0.66 ± 0.22	1.17 ± 0.24
LDI/LDI$_{extract}$	309	0.27 ± 0.11	0.83 ± 0.31	648	0.29 ± 0.11	0.72 ± 0.24
All	430	0.48 ± 0.15	1.07 ± 0.31	817	0.49 ± 0.15	0.93 ± 0.26

*LDI$_{extract}$: LDI performed on extract used for ESI analysis; **LDI: direct LDI imaging of filters

Fig. S9. Overlap in molecular compositions delineated from negative-ion laser desorption (LDI) or (-)LDI$_{extract}$ and/or electrospray ionisation / 15-T FT-ICR MS analyses of BBAug1011 and BBAug1314 in the van Krevelen space. The associated table presents averages of O/C and H/C weighted to abundance for entire datasets. The bottom panel of this table in grey presents the number averages of ionisation methods as more than species common to ≥2 methods are being compared.
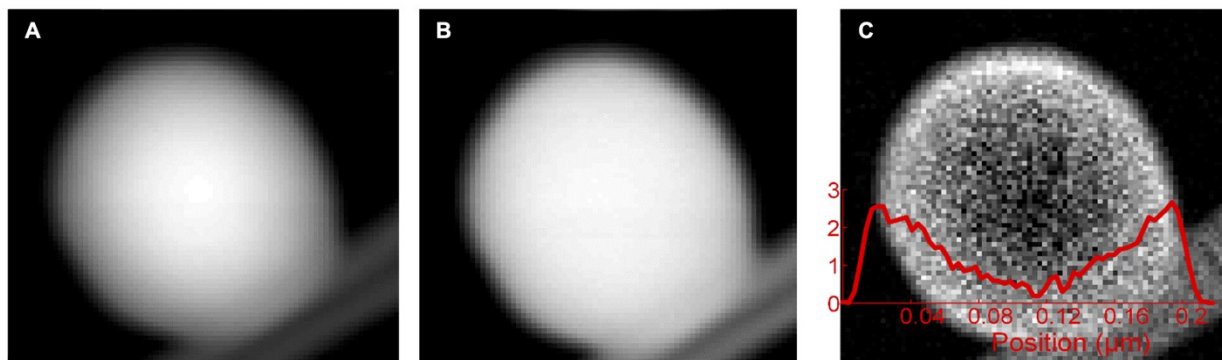
Fig. S10 Single-particle analysis on tar balls (TBs) showing the distribution of carbon and oxygen in a representative TB, (A) Scanning transmission electron microscopy (STEM) image of a TB in BBAug1314, (B) STEM/ electron energy loss spectrometry (EELS) image showing homogenous distribution of carbon within TB particle, (G) STEM/EELS image showing the abundance of O in the extremities of TB with a sequential decrease toward the centre of the TB.
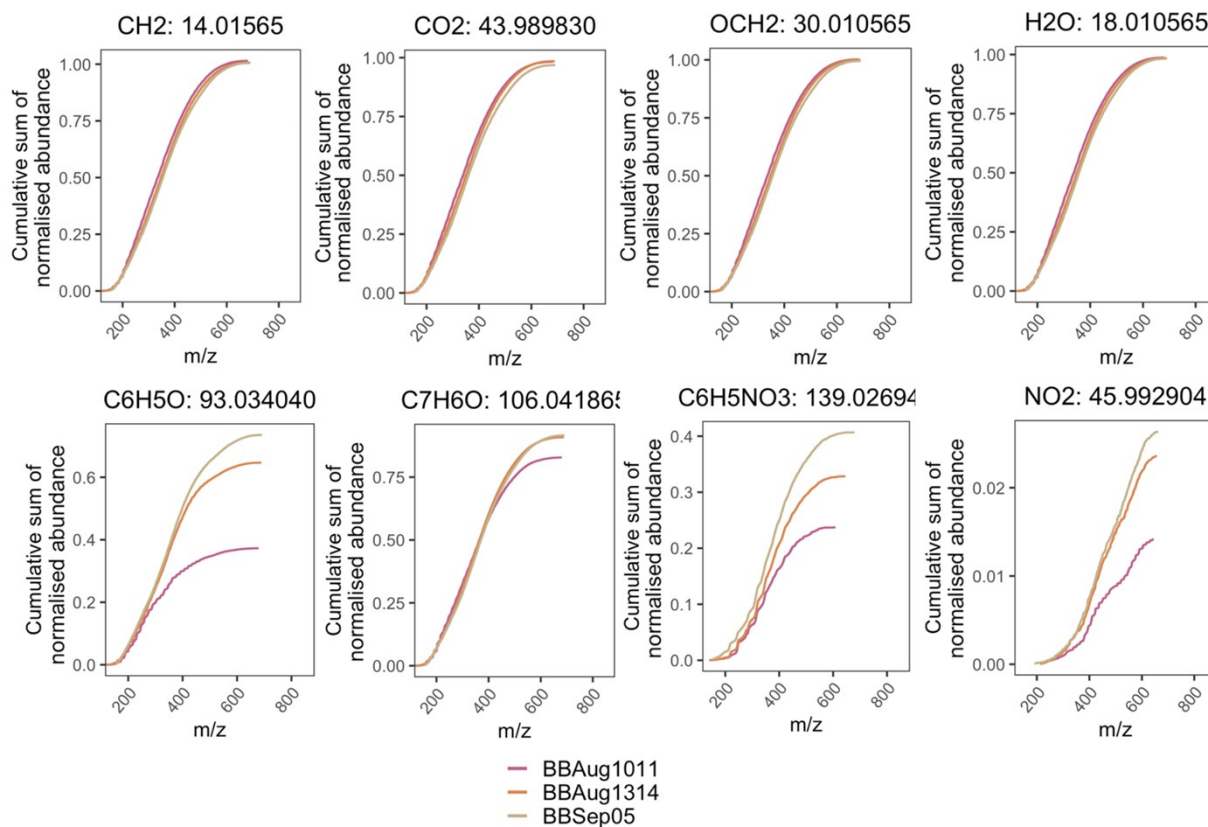

Fig. S11 A comparison of the contribution of a variety of aromatic and non-aromatic functional units to the ion abundance in TB-rich (BBSep05 and BBAug1314) and TB-poor samples (BBAug1011) as determined from their presence in Kendrick mass defect homologous series calculated using these moieties as the KMD bases in molecular composition from negative-ion electrospray ionisation / 15-T FT-ICR MS analysis.

R CODE USED FOR FORMULA ASSIGNMENT WITH MFASSIGNR[6]

Key settings (to be defined by the user) are highlighted in bold and blue or orange for (-)ESI and (-)LDI, respectively.

Step 1: Load libraries
library(MFAssignR)

Step 2: Set the working directory and read the data

Step 3: Estimate noise
Noise <- KMDNoise(Data, upper.y = 0.52, lower.y = 0.07, upper.x = NA, lower.x = NA)
plot <- Noise[["KMD"]]
plot
KMDN <-Noise[["Noise"]]

Step 4: Isotope pre-screening
Isotopes <- IsoFiltR(Data, **SN = 1.7*KMDN, Carbrat = 60, Sulfrat = 30, Sulferr = 1.2, Carberr = 1.2**)
OR
Isotopes <- IsoFiltR(Data, **SN = 0*KMDN, Carbrat = 60, Sulfrat = 30, Sulferr = 2, Carberr = 2**)
Mono <- Isotopes[["Mono"]]
Iso <- Isotopes[["Iso"]]

Step 5: Preliminary CHO assignments to pick recalibrants
Assign <- MFAssignCHO_RMD(Mono, Iso, ionMode = "neg", SN = **1.7*KMDN**, **ppm_err = 1.5**, H_Cmin = 0.3, H_Cmax = 2.5, O_Cmax = 2.0, DBEOmax = 20, DBEOmin = -13, **NMScut = "on", DeNovo = 1000**, highMW = 1200, lowMW = 100)
OR
Assign <- MFAssignCHO_RMD(Mono, Iso, ionMode = "neg", **SN = 0*KMDN, ppm_err = 2**, H_Cmin = 0.0, H_Cmax = 2.5, O_Cmax = 2.0, **DBEOmax = 80**, DBEOmin = -13, NMScut = "on", **DeNovo = 1000,** highMW = 1200, lowMW = 100)
Unambig1.temp <- Assign[["Unambig"]]
Unambig1 <- Unambig1.temp %>% arrange(desc(abundance)) %>% distinct(formula, .keep_all = TRUE)
Ambig1 <- Assign[["Ambig"]]
Unassigned1 <- Assign[["None"]]
MSAssign_CHO <- Assign[["MSAssign"]]
Error_CHO <- Assign[["Error"]]
MSgroups_CHO <- Assign[["MSgroups"]]
VK_CHO <- Assign[["VK"]]

Step 6: Mass recalibration
RecalList <- RecalList(df = Unambig1)
Recalibration <- Recal(Unambig1, peaks = Mono, isopeaks = Iso, mode = "neg", **mzRange = 20, SN = 1.7*KMDN, series1 = "O3_H_5", series2 = "O7_H_4", series3 = "O9_H_9", series4 = "O13_H_11", series5 = "O15_H_13", series6 = "O18_H_11", series7 = "O18_H_13", step_O = 3, step_H2 = 5**)
OR
Recalibration <- Recal(Unambig1, peaks = Mono, isopeaks = Iso, mode = "neg", **mzRange =25, SN = 0*KMDN, series1 = "O6_H_5", series2 = "O10_H_10", series3 = "O9_H_11", series4 = "O7_H_9", series5 = "O11_H_10", series6 = "O12_H_15", series7 = "O13_H_14", series8 = "O5_H_3", step_O = 3, step_H2 = 5**)
Plot_Recalibration <- Recalibration[["Plot"]]
Plot_Recalibration
Mono2 <- Recalibration[["Mono"]]
Iso2 <- Recalibration[["Iso"]]
List <- Recalibration[["RecalList"]]

Step 7: Final formula assignment – Round 1
Assign <- MFAssign_RMD(peaks = Mono2, isopeaks = Iso2, lowMW = 100, highMW = 1200, ionMode = "neg", **SN = 1.7*KMDN, ppm_err = 0.5, iso_err = 0.5,** H_Cmin = 0.3, O_Cmax = 2.0, H_Cmax = 2.5, DBEOmax = 20, DBEOmin = -13, HetCut = "off", **NMScut = "on", DeNovo = 1000, SulfCheck = "on", Ambig = "off", MSMS = "off", N3corr = "on"**)
OR

Assign <- MFAssign_RMD(peaks = Mono2, isopeaks = Iso2, lowMW = 100, highMW = 1200, ionMode = "neg", **SN = 0*KMDN, ppm_err = 0.5, iso_err = 0.5**, H_Cmin = 0.0, O_Cmax = 2.0, H_Cmax = 2.5, DBEOmax = 80, DBEOmin = -13, **HetCut = "off", NMScut = "on", DeNovo = 1000, SulfCheck = "on", Ambig = "off", MSMS = "on", N3corr = "on", NOEx = 1**)
Unambig2 <- Assign[["Unambig"]]
Ambig2 <- Assign[["Ambig"]]
Unassigned2 <- Assign[["None"]]
MSAssign_MF <- Assign[["MSAssign"]]
Error_MF <- Assign[["Error"]]

Step 8: Final formula assignment – Round 2
Isotopes.2 <- IsoFiltR(Unassigned2, **SN = 0*KMDN, Carbrat = 60, Sulfrat = 30, Sulferr = 0.5, Carberr = 0.5**)
Mono3 <- Isotopes.2[["Mono"]]
Iso3 <- Isotopes.2[["Iso"]]
Assign.2 <- MFAssign_RMD(peaks = Mono3, isopeaks = Iso3, lowMW = 100, highMW = 1200, ionMode = "neg", **SN = 0*KMDN, ppm_err = 0.5, iso_err = 0.5**, H_Cmin = 0.3, O_Cmax = 2.0, H_Cmax = 2.5, DBEOmax = 20, DBEOmin = -13, **HetCut = "off", NMScut = "on", DeNovo = 350, SulfCheck = "on", Ambig = "off", MSMS = "off", N3corr = "on", Nx = 3, Sx = 1**)
OR
Assign.2 <- MFAssign_RMD(peaks = Mono3, isopeaks = Iso3, lowMW = 100, highMW = 1200, ionMode = "neg", **SN = 0*KMDN, ppm_err = 0.5, iso_err = 0.5**, H_Cmin = 0.0, O_Cmax = 2.0, H_Cmax = 2.5, DBEOmax = 80, DBEOmin = -13, **HetCut = "off", NMScut = "on", DeNovo = 350, SulfCheck = "on", Ambig = "off", MSMS = "on", N3corr = "on", Nx = 3, Sx = 1, NOEx = 1**)
Unambig3 <- Assign.2[["Unambig"]]
Ambig3 <- Assign.2[["Ambig"]]
Unassigned3 <- Assign.2[["None"]]
MSAssign_MF <- Assign.2[["MSAssign"]]
Error_MF <- Assign.2[["Error"]]
MSgroups_MF <- Assign.2[["MSgroups"]]

Step 9: Combine output from step 7 (CHO assignments only) and step 8 (N and S containing assignments)

Step 10: User-specific data cleaning and plotting

SELECTIVE CO-ADDITION OF TRANSIENTS FROM LDI-IMAGING MODE DATA

1. For each dataset, the total ion current (TIC) for each pixel was extracted from the 'ImagingInfo.xml' file.
2. For each dataset, TIC thresholds (min, max) were empirically defined to yield an optimal signal quantity and quality. These ranges varied from $2.2 \times 10^9 - 2.4 \times 10^9$ to $2.7 \times 10^9 - 2.9 \times 10^9$, typically covering only a narrow 2×10^8 range of TIC values. These values were chosen based on an examination of the distribution of TIC values and an inspection of the signal quality within those bounds (based on subsequent steps).
3. For each dataset, 48 transients were selected from within those TIC bounds and co-added prior to typical processing (i.e. apodisation, zero filling, Fourier transform).
a. The transients were read from the *ser* file in binary format with datatype *int32*.
b. Apodisation was performed with a Hamming function.
c. Two zero-fills were performed.
d. Magntiude-mode data were produced from the absolute value of the real fast Fourier transformation.
e. Frequency-to-mass conversion was performed with a 3-term Ledford equation using the instrument coefficients: ML1, ML2, ML3.
f. Visual inspection of the spectra – examining line shape quality, signal-to-noise, etc. – was used to assess if the TIC bounds were appropriate; they were iteratively refined until sufficiently high-quality spectra were obtained.
4. The mass spectrum was imported into CoreMS for internal recalibration, noise thresholding, and peak picking.
a. A linear recalibration was performed using endogenous homologous CHO series.
b. Peaks were picked using the 'minima' method of CoreMS with a threshold of standard deviations.
c. Peaks were exported to text files for further analysis.

REFERENCES

1. B. Koch and T. Dittmar, *Rapid Comm Mass Spectrometry*, 2006, **20**, 926-932.
2. B. P. Koch and T. Dittmar, *Rapid Comm Mass Spectrometry*, 2016, **30**, 250-250.
3. Y. Li, U. Pöschl and M. Shiraiwa, *Atmos. Chem. Phys*, 2016, **16**, 3327-3344.
4. W.-S. W. DeRieux, Y. Li, P. Lin, J. Laskin, A. Laskin, A. K. Bertram, S. A. Nizkorodov and M. Shiraiwa, *Atmospheric Chemistry and Physics*, 2018, **18**, 6331-6351.
5. M. Shiraiwa, Y. Li, A. P. Tsimpidi, V. A. Karydis, T. Berkemeier, S. N. Pandis, J. Lelieveld, T. Koop and U. Pöschl, *Nature communications*, 2017, **8**, 1-7.
6. S. K. Schum, L. E. Brown and L. R. Mazzoleni, *Environmental Research*, 2020, **191**, 110114.